Multifractality In Arterial Pulse

Aniruddha J. Joshi, Sharat Chandran
Computer Science and Engg. Dept., IIT Bombay, Powai, Mumbai, India 400076
ajjoshi@cse.iitb.ac.in
V. K. Jayaraman, B. D. Kulkarni
Chemical Engineering and Process Development Division, National Chemical Laboratory, Pune, India 411008

Abstract

Extensive research has been done to show that heartbeats are composed of the interaction of many physiological components operating on different time scales, with nonlinear and self-regulating nature. The more direct, and easily accessible manifestation of the heartbeat is the pulse; however, it has not been studied anywhere near as extensively.

*In this paper, we establish the relevance of the multifractal formalism for the arterial pulse, which has long been used as a fundamental tool for diagnosis in the Traditional Indian Medicine, (*Ayurveda*). The finding of power-law correlations through detrended fluctuation analysis indicates presence of scale-invariant, fractal structures in the pulse. These fractal structures are then further established by self-affine cascades of beat-to-beat fluctuations revealed by wavelet decomposition at different time scales. Finally, we investigate how these pulse dynamics change with age, and disorder. The analytic tools we discuss may be used on a wide range of physiological signals.*

1 Introduction

Beat-to-beat variations of the heart (and other physiological signals) are members of a special class of complex processes — those which are inhomogeneous, nonstationary, and display multifractal properties [11, 10]. In contrast to the electrocardiogram (ECG), and despite thought of being similar, the arterial pulse has not been extensively studied. The principal reason, it would appear, that the pulse has not yet received due scientific recognition is the lack of quantitative basis. We have developed a data acquisition system named *Nadi Tarangini* [13] for obtaining clean, and accurate pulse waveforms. It incorporates pressure transducers, an ADC, and storage and analysis capabilities. A sample waveform is shown in Figure 1. The differences between the peaks (778, 832 and so on) form the pulse beat-to-beat time series.

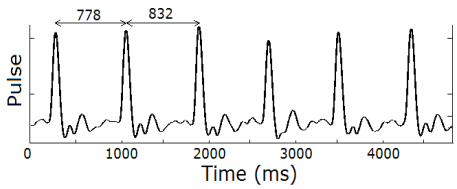

Figure 1. A sample of the pulse waveform from our *Nadi Taringini* system [13].

Historically, the pulse has in fact been extensively used in diagnosis. The *Indian Traditional Medicine* believes that the function of entire human body is governed by three humors: *Vata* (V), *Pitta* (P), and *Kapha* (K), collectively termed as *Tridosha* [19] and represented as *VPK*. The imbalance in these causes the vessels carrying the blood to contract or expand with respect to its normal position. This contraction & expansion of vessels results in modulation of blood flow, which is termed as the *nadi* or pulse [19]. Thus, studying a large amount of information from the pulse can lead one to an improved understanding of the disease process affecting a patient.

Traditional Chinese Medicine (TCM) also uses similar diagnostic procedures [2]. Researchers have already started obtaining pulse waveforms and apply modern research techniques on these spectra with reference to the TCM; such as analyzing pulse waveforms with variations in age [6] [4], gender [6], and diagnosis of severe liver problems [15].

Our contribution: This work may be viewed as consisting of three parts

- Like the beat-to-beat variations of the heart, we show – to our knowledge for the first time – that the arterial pulse also exhibits self-similar nature and requires a large numbers of exponents to characterize their scaling properties.
- We show that the detrended fluctuation analysis

(DFA) technique (see §2) indicates the presence of scaling (self-similarity) through a linear relationship on a log-log graph, such that fluctuations in small boxes are related to the fluctuations in larger boxes in a power-law fashion. To better quantify the nature of these waveforms, we turn to the wavelet transform modulus maxima (WTMM) based multifractal formalism, and show that the pulse requires not one but many exponents to fully characterize the scaling properties.

- With aging and disease, fractal structures may show degradation in their structural complexity [14]. We show that our multifractal spectrums vary for pulses from three age-groups and two disorders as shown in Figure 5. Naturally, this provides better diagnoses capabilities.

The rest of the paper is organized as follows. The method of DFA described in §2 establishes the self-similarity nature. Therefore the multifractal analysis was conducted, and is described in §3 along with experimental results. A discussion with our final remarks follows in §4.

2 Detrended Fluctuation Analysis

To illustrate the DFA algorithm [9] briefly, consider the pulse beat-to-beat series $f(i)$ $[i = 0, \ldots, N-1]$ shown in Figure 2 (a). First, f is suitably integrated $y(k) = \sum_{i=0}^{k-1}(f(i) - M)$ where M is the mean. (Notice that values of $f(i) - M$ are signed.) $y(k)$ is now divided into boxes of equal width n and the least-square line fitting the data in each box, $y_{p,n}(j)$,

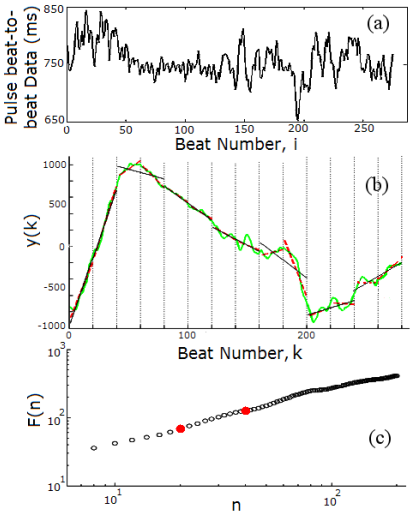

Figure 2. (a) Pulse beat-to-beat data. (b) $y(k)$ (in green), and local trends for $n = 20$ (in red) and $n = 40$ (in black). (c) Log-log plot of $F(n)$ versus n shows a linear trend.

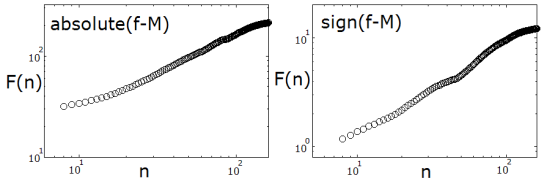

Figure 3. Linear plots for absolute and sign values.

$j = 0 \ldots (N/n) - 1$, $p = 1 \ldots n$, is computed. The integrated time series is then detrended by subtracting the local trend $y_{p,n}(j)$, and the root-mean square fluctuation of the entire detrended series, $F(n)$ is computed

$$F(n) = \sqrt{(\frac{1}{N}\sum_{k=0}^{N}[y(k) - y_{p,n}(\lfloor k/n \rfloor)]^2)} \quad (1)$$

2.1 Self-similarity in Pulse

As shown in Figure 2 (b), $y(k)$ is the solid green curve and the vertical dotted lines indicate boxes of width $n = 20$. The red and black straight line segments represent the *trends* estimated in each box of sizes $n = 20$ & $n = 40$ respectively by a linear least-squares-fit. Note that the typical deviations for the two lines is different. $F(n)$ is now plotted against the box width n for various values in Figure 2 (c). The two highlighted points in red are for $n = 20$ & $n = 40$.

Typically, $F(n)$ increases with box size n. The linear relationship on a log-log graph (Figure 2 (c)) indicates the presence of power-law scaling (self-similarity), such that fluctuations in small boxes are related to the fluctuations in larger boxes in a power-law fashion. The slope of the line relating $\log(F(n))$ to $\log(n)$ determines the fractal scaling exponent.

2.2 DFA on absolute and sign values

Similar self scaling is also observed if we take absolute values (i.e., $|f - M|$) as shown in Figure 3 (a). A similar nature is found if $f - M$ is approximated to be a binary number (1 or -1). This situation has been previously explored for beat-to-beat patterns of ECG [10].

3 Multifractal Spectrum

In our work, we have applied the wavelet-based multifractal spectrum approach for feature extraction from the pulse beat-to-beat signal. The continuous wavelet transform (CWT) of a function f $(W(f))$ is a convolution product of the time series with a scaled and translated kernel. In our work, we used derivatives of the Gaussian function ("Mexican hat wavelets"). Their time-frequency localization properties make them particularly useful for the task of revealing the underlying hierarchy that governs the temporal distribution of the local Hurst exponents [16].

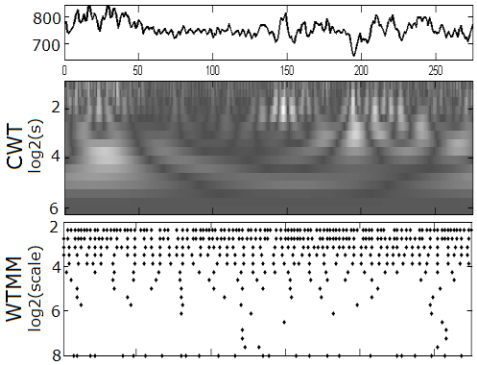

Figure 4. A sample pulse waveform and the corresponding WTMM tree.

As the CWT is an extremely redundant and a computationally expensive representation, the WTMM method [8] changes the continuous sum over space into a discrete sum by taking the local maxima. The branching structure of the WTMM skeleton in the (scale,time) plane indicates the hierarchical organization of the singularities. This is clearly illustrated in Figure 4.

The WTMM method consists in taking advantage of the space-scale partitioning given by this skeleton to define a series of exponents $\tau(q)$ through the following partition functions $Z(s,q)$ of q^{th} moment based on multifractal formalism [3] [16]:

$$Z(s,q) = \sum_{\Omega(s)} |W(f)|^q \propto s^{\tau(q)} \qquad (2)$$

where $\Omega(s)$ is the set of all maxima at the scale s. Here, q has the ability to select a desired range of values. The scaling function $\tau(q)$ globally captures the distribution of the exponents h. For large negative q, weak exponents are addressed, while strong exponents are effectively filtered out; at the same time, for large positive q, the opposite situation is in place [11]. This dependence could have a slope non-linearly changing with q. The local tangent slope to $\tau(q)$ gives the corresponding exponent $h(q)$. The related dimensions $D(h)$ for each value of h form the spectrum of singularities of the signal. Formally, the transformation from $\tau(q)$ to $D(h)$ is referred to as the Legendre transformation [3]:

$$h(q) = d\tau(q)/\,dq \qquad (3)$$

$$D[h(q)] = q\,h(q) - \tau(q) \qquad (4)$$

3.1 Results

The pulse waveforms were recorded using *Nadi Tarangini* [13]. There are 6 pulse waveforms for each volunteer corresponding to the three pick-up positions (*VPK* at the root of thumb on wrist) on two hands [19]. In this study, we had a total of 108 waveforms from 16 volunteers with *no disorder*. (Some volunteers were recorded multiple times).

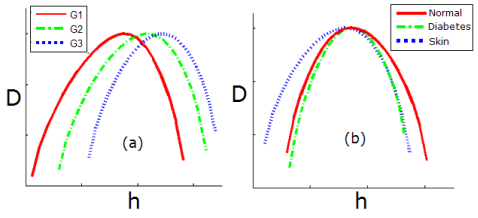

Figure 5. Variations in spectra for (a) normal subjects and for 3 age-groups (b) Group (G3) spectra with normal subjects, subjects with diabetes (green), and subjects with skin abnormalities (blue).

We extracted peaks in these signals using a complex frequency b-spline wavelet [12]. The length of each waveform is at least 250, and the distances in them form the pulse beat-to-beat time series. We obtained the multifractal spectra for all the signals in the database using the methodology explained in § 3 and adapting the Legendre spectrum code from FracLab [1].

Variations with Age: Figure 5 (a) shows the results. The results are grouped according to age into three groups– 'less than 25' (G1), '25 to 50' (G2) and 'above 50' (G3) respectively. The spectra from the left hand of the *vata* pulse vary, as shown in Figure 5 (a). We observe that the multifractal spectrum drifts to higher values of h, as the age increases. (Only the average case is drawn for better visibility.) The results for other pick-up positions on both hands also show similar behavior, but are not displayed in this paper due to space restrictions.

Variations with Disorder: Figure 5 (b) shows the results. In this case, the multifractal spectra of volunteers in the age group G3 has been chosen. Three of these volunteers had diabetes, five had problems with skin, and three were normal (i.e., no complaints). It can be seen that the spectra vary, and hence there is an opportunity for classification. These spectra were for the nadi taken with the left hand and the *vata* position; but again, similar behaviour was observed for all pick-up positions.

4 Discussion and Final Remarks

The signal characteristics of the arterial pulse has not been as thoroughly investigated in the community. In this paper, we showed the presence of self-similarity scaling in arterial pulse data through a linear relationship on a log-log graph in DFA analysis. Also, we studied the fractal characteristics of pulse beat-to-beat signals with the multifractal formalism based on the WTMM method. The spectra showed variations in range and area depending upon age and disorder of the person in both the hands, and also for locations *VPK*. Our results (to our knowledge for the first time for the arterial pulse) are consistent with the behaviour re-

	Left Hand			Right Hand		
	G1	G2	G3	G1	G2	G3
Normal	14.95	15.23	14.82	15.04	15.40	13.71
Diabetes	–	–	14.36	–	–	15.27
Skin	13.67	–	14.25	14.82	–	13.47

Table 1. Area ratios for multiple age groups, and varying disorders.

ported for ECG signals. Multifractal studies have been undertaken in other domains such as DNA sequences [18], turbulence [5], day and night heart rate characteristics [17], alterations with disease and aging [7].

In this study, we have confined our scope to extract only the multifractality present in the pulse waveforms. The results in Section 3.1 are consistent with the heartbeat results from [20], which states that a person's multifractal spectrum is controlled mainly by his neurosystem. With advancing age, the neuroautonomic control of people's body on the ECG decreases and tends from multifractality to monofractality. We provide the ratios of areas under the spectra in the Table 1. It can be observed that the areas under G2 have higher values as compared to those under G3. And it reinforces the assumption of [11].

The varying ranges of the $D(h)$ curve (Figure 5) for various disorders may be useful for classification of various types of nadi. Also, the nadi signal (obtained from convenient, inexpensive, painless, and noninvasive *Nadi Tarangini*) identifies the presence and location of disorders in a patients body [19], unlike ECG which mainly reflects the electrical activity of the heart, and thus the pulse contains much more useful information than ECG. Therefore, a diagnostic system can be formed using these multifractal values (and other informative features from the pulse signals) and providing them as input vectors to a classifier (e.g. multiclass Support Vector Machine). Further detailed studies on a larger number of datasets are needed to establish the advantages of the given method compared to others and to find optimal combinations of methods for diagnostic and prognostic purposes.

References

[1] http://complex.futurs.inria.fr/fraclab/. Last viewed on Feb 10, 2008.

[2] http://www.naturalhealthweb.com/articles/nations-weissman3.html. Last viewed on March 19, 2008.

[3] A. Arneodo, E. Bacry, and J. Muzy. The thermodynamics of fractals revisited with wavelets. *Physica A*, 213:232–275, 1994.

[4] A. Brumfield and M. Andrew. Digital pulse contour analysis: investigating age-dependent indices of arterial compliance. *Physiological Measurement*, 26:599–608, 2005.

[5] A. Chhabra, C. Meneveau, R. Jensen, and K. Sreenivasan. Direct determination of the $f(\alpha)$ singularity spectrum and its application to fully developed turbulence. *Physical Review A*, 40:5284–5294, 1989.

[6] S. Christopher and P. Raymond. Gender-related differences in the central arterial pressure waveform. *American College of Cardiology*, 30:1863–1871, 1997.

[7] A. Goldberger, L. Amaral, J. Hausdorff, P. Ivanov, C. Peng, and H. Stanley. Fractal dynamics in physiology: Alterations with disease and aging. In *National Academy of Sciences, USA*, volume 99, pages 2466–2472, 2002.

[8] W. Hwang and S. Mallat. Characterization of self-similar multifractals with wavelet maxima. *Applied and Computational Harmonic Analysis*, 1:316–328, 1994.

[9] P. Ivanov, L. Amaral, A. Goldberger, S. Havlin, M. Rosenblum, H. Stanley, and Z. Struzik. From 1/f noise to multifractal cascades in heartbeat dynamics. *Chaos*, 11:641–652, 2001.

[10] P. Ivanov, Z. Chen, K. Hu, and H. Stanley. Multiscale aspects of cardiac control. *Physica A*, 344:685–704, 2004.

[11] P. Ivanov, M. Rosenblum, L. Amaral, Z. Struzik, S. Havlin, A. Goldberger, and H. Stanley. Multifractality in human heartbeat dynamics. *Nature*, 399:461–465, 1999.

[12] A. Joshi, S. Chandran, V. Jayaraman, and B. Kulkarni. Arterial pulse system: modern methods for traditional indian medicine. In *29th Annual International Conference of the IEEE Engineering in Medicine and Biology Society*, pages 608–611, 2007.

[13] A. Joshi, A. Kulkarni, S. Chandran, V. Jayaraman, and B. Kulkarni. Nadi tarangini: a pulse based diagnostic system. In *29th Annual International Conference of the IEEE Engineering in Medicine and Biology Society*, pages 2207–2210, 2007.

[14] L. Lipsitz and A. Goldberger. Loss of "complexity" and aging: Potential applications of fractals and chaos theory to senescence. *American Medical Association*, 267:1806–1809, 1992.

[15] W. Lu, Y. Wang, and W. Wang. Pulse analysis of patients with severe liver problems. *IEEE Engineering in Medicine and Biology Magazine*, 18:73–75, 1999.

[16] J. Muzy, E. Bacry, and A. Arneodo. The multifractal formalism revisited with wavelets. *International Journal of Bifurcation and Chaos*, 4:245–302, 1994.

[17] S. Ramchurn and A. Murray. Multifractal analysis of the day and night characteristics of heart rate variability. *Computers in Cardiology*, pages 421–424, 2002.

[18] L. Rossi and G. Turchetti. Poincaré recurrences and multifractal properties of genomic sequences. *Physica A*, 338:267–271, 2004.

[19] S. Upadhyaya. *Nadi Vijnana (Ancient Pulse Science)*. Chaukhamba Sanskrit Pratishthan, 1999.

[20] J. Wang, X. Ning, and Y. Chen. Multifractal analysis of electronic cardiogram taken from healthy and unhealthy adult subjects. *Physica A*, 323:561–568, 2003.